Modeling the Free Energy Landscape for Janus Particle Self-Assembly in the Gas Phase

Andrew W. Long and Kridsanaphong Limtragool

Abstract

The self-assembly of Janus particles into vesicle-type structures is an important process in the development of novel "smart" drug delivery techniques. Understanding the energetics and barriers to vesicle formation from particles in the dilute gas phase will help drive researchers to tailor synthesis parameters. We propose a combination of canonical ensemble Monte Carlo with umbrella sampling to efficiently sample the phase space for self-assembly, and reconstruct the free energy landscape for self-assembly using the weighted histogram analysis method. From this initial work, we characterize the activation barrier for formation of micelles from particles in the gas phase and see a spontaneous driving force for micelle aggregation and reconfiguration into vesicles. By comparing the self-assembly landscape across different temperatures and densities of particles in the gas phase, we can determine basic design rules to minimize the barrier to formation and increase the propensity for vesicle formation.

1 Introduction

The self-assembly mechanisms for Janus particles is of interest both as a coarse-grained model for surfactant molecules and for novel applications in colloid science. Janus type interactions can be realized experimentally, where different sections of a particle are patterned with different materials to produce anisotropic behavior. These systems can be made in such a way that their assembly behavior is analogous to lipids in solution, with hydrophobic and hydrophillic functionalization, allowing for the development of interesting colloidal structures such as self-assembled bilayers and vesicles. Understanding the mechanisms by which Janus particles assemble would allow for the design of drug encapsulating vesicles that self-assemble in solution, and understanding the energetics of such structures could help researchers effectively design triggers for vesicle disassembly and drug delivery.

Work done previously by Sciortino et al. [1] has investigated the gas-liquid phase diagram for spherical Janus particles with a single attractive hemisphere, while the other hemisphere remains inert. In this work, they observe the formation of vesicles in the gas phase through a three-stage process. First, free particles in the gas must aggregate into micelle type structures, with sizes of approximately 10 colloidal particles. Next, a series of micelles must coalesce, forming an energetically unfavorable tubular structure, which will finally rearrange itself into the desired low energy vesicle shape. We look to investigate this multistage assembly process by modeling the free energy landscape on which these structures reside.

In order to generate the free energy landscape for self-assembly, we will utilize the umbrella sampling technique in order to effectively bias our simulations. This technique has been used extensively in the literature looking to bias simulations of Lennard Jones systems to understand nucleation phenomena in the gaseous phase [3][4]. These works utilize a cluster order parameter of

rotationally invariant spherical harmonics that characterizes the local symmetry of particles, varying between random particles in the gas to highly ordered nucleated clusters [5]. We look to simplify this process by looking at a bond order parameter that mimics this cluster order parameter, without having to solve for the cluster that each particle belongs to and the effect of particle movement on the global cluster order parameter. This will allow for a much faster algorithm, however, care will need to be taken to ensure the bond-order parameter can effectively encapsulate the structures of interest.

2 Methods

2.1 Particle Model

In this work we use the Kern-Frenkel model to describe our Janus Particles [1]. In this model, each particle has a single hemispheric attractive patch characterized by a unit patch vector $\hat{n}_i$ that points in the direction of the patch center. Particle-particle interactions are defined as hard-sphere at all length scales below the particle diameter. Beyond this range, an orientational square-well potential is used as defined in equations (1-3).

$$V(\vec{r}_{ij}) = v^{sw}(\vec{r}_{ij}) f(\vec{r}_{ij}, \hat{n}_i, \hat{n}_j) \tag{1}$$

$$v^{sw}(\vec{r}_{ij}) = \begin{cases} \infty & \text{if } |\vec{r}_{ij}| < \sigma \\ -\epsilon, & \text{if } \sigma \leq |\vec{r}_{ij}| \leq \sigma + \Delta \\ 0, & \text{if } |\vec{r}_{ij}| > \sigma + \Delta \end{cases} \tag{2}$$

$$f(\vec{r}_{ij}, \hat{n}_i, \hat{n}_j) = \begin{cases} 1, & \text{if } \vec{r}_{ij} \cdot \hat{n}_i \geq 0 \text{ and } \vec{r}_{ji} \cdot \hat{n}_j \geq 0 \\ 0, & \text{else} \end{cases} \tag{3}$$

This orientational factor as defined by equation (3) corresponds to the vector that connects the two particles passing through the attractive patches on each particle, effectively defining the state where the attractive patches on the particles are facing one another. In this work, we use $\Delta = 0.5\sigma$, which for a system of nano particles can be realized experimentally.

2.2 Free Energy Landscape

The free energy landscape along a reaction coordinate ξ is defined as

$$A(\xi) = -\frac{1}{\beta} \ln Z(\xi) \tag{4}$$

Where $Z(\xi)$ is defined as

$$Z(\xi) = \frac{\int \delta(\xi(r) - \xi) \exp(-\beta E) d^N r}{\int \exp(-\beta E) d^N r} \tag{5}$$

This function $Z(\xi)$ can be obtained from the distribution of our order parameter ξ across simulation trajectories. A simple reconstruction of the free energy landscape can be made by generating a trajectory, sampling ξ along the trajectory, solving for the distribution $Z(\xi)$ through histogramming, and then this distribution can be used in the above equation to solve for the free energy. The issue with such a naïve approach comes from the fact that simulations tend to reside in local equilibrium points. By directly sampling our reaction coordinate, non-equilibrium positions will effectively be undersampled, drastically affecting the free energy barriers between possible meta-stable configurations.

2.3 Umbrella Sampling

To circumvent this issue, simulations must be biased in order to effectively sample each region of the reaction coordinate. In umbrella sampling, we selectively bias our simulation trajectories along a reaction coordinate by the use of an additional term in the potential calculation [6]. We can define the total energy U for a particle in this biased regime as:

$$U(s_i) = V(s_i) + \alpha(s_i) \tag{6}$$

Where s_i is the state of the ith particle, V is the potential due to particle-particle interactions, and α is our biasing function. We utilize a harmonic bias potential for α, with the form

$$\alpha(s_i) = k_B T \frac{\kappa}{2}(\xi(s_i) - \xi_0)^2 \tag{7}$$

with ξ_0 being the specific reaction coordinate to bias our trajectory at, $\xi(s_i)$ is the reaction coordinate for particle i, and κ is the strength of our biasing function. Larger values for κ correspond to narrow distributions of the particle reaction coordinate around the biasing coordinate, as the relative contribution to the particle energy will be greater. The selection of κ must be made to allow for overlap between our biasing trajectories in order to get a smooth surface from the WHAM algorithm described later. This biased energy term can be used in our Monte Carlo acceptance criteria. As our probability of selecting a transition between state s_i and s_i' is symmetric, the acceptance criteria can be written as

$$acc(s_i \to s_i') = \min\{1, \exp(-\beta\Delta V)\exp(-\beta\Delta\alpha)\} \tag{8}$$

which allows us to sample a trajectory following the new energy parameter. Along our simulation, we tabulate values of the reaction coordinate for all particles to be used in reconstructing the free energy landscape along our coordinate using WHAM.

2.4 Bond Order Parameter

For this work, we look at using the bond order parameter Q_4, a sum of rotational invariant spherical harmonics calculated as

$$Q_4^i \equiv \left[\frac{4\pi}{9}\sum_{m=-4}^{4}|\bar{Q}_{4m}^i|^2\right]^{1/2} \tag{9}$$

$$\bar{Q}_{4m}^i \equiv \frac{1}{N_{neigh}}\sum_{r_{ij}<\sigma+\Delta} Y_{4m}(r_{ij}) \tag{10}$$

Where r_{ij} is the bond vector between particles i and j, and the sum runs across all neighboring particles N_{neigh} within the well depth (irrespective of bonding with particle i). This gives a local measure of the symmetry around a particle, with a Q_4 value of zero for a particle that is spherically surrounded by its neighbors, and a Q_4 of one for a free particle in solution. This bond order parameter has been extensively used in nucleation theory for Lennard-Jones system [3][4] and other self-assembly systems.

2.5 Weighted histogram analysis method (WHAM)

Once the distribution of the reaction coordinate has been sampled over a series of windows, the free energy landscape can be reconstructed. In order to account for the bias used in each windowed simulation, the weighted histogram analysis method can be used to effectively unbias the distribution of the reaction coordinate. The WHAM algorithm works by trying to find weights p_i for each window that minimize the error in our calculation of $P^u(\xi)$, or equivalently, finding weights that maximize the expected likelihood of our data.

$$P^u(\xi) = \sum^{windows} p_i(\xi) P_i^u(\xi) \tag{11}$$

In order to find these weights, an expectation maximization (EM) technique is used. The EM algorithm is a standard iterative method in statistics for estimating model parameters in a self-consistent manner. The E-step calculates $P^u(\xi)$ from the selected weights as defined above, starting from an initial guess of equal weights between all windows. The M-step updates the weights by first approximating the shift constants for each window F_i as

$$\exp(-\beta F_i) = P^u(\xi) \int \exp\left[-\beta \alpha_i(\xi)\right] d\xi \tag{12}$$

The weights for each window are then calculated as (noting that $\sum p_i = 1$)

$$p_i = \frac{N_i \exp\left[-\beta \alpha_i(\xi) + \beta F_i\right]}{\sum_j N_j \exp\left[-\beta \alpha_j(\xi) + \beta F_j\right]} \tag{13}$$

Where N_i is the number of points sampled in the ith window, and α_i is the harmonic potential for the sampled window as above. These updated weights are used in the next iteration's E-step, and this iteration scheme is continued until a desired tolerance in the error is reached. After completion of the EM algorithm, the unbiased distribution $P^u(\xi)$ has been reconstructed, and the free energy landscape can be generated.

2.6 Simulation Details

In this work, we simulate our system with canonical ensemble Metropolis Monte Carlo using 64 particles our simulation box with periodic boundary conditions for a variety of system densities and temperatures. We set the simulation length scale and energy scale to be the particle diameter and square-well strength respectively, ie. $\sigma = 1$ and $\epsilon = 1$. Additionally, we measure the temperature in reduced units where $k_B = 1$. Possible moves are translation of particle centers and rotations of the patch vectors around these centers. These moves are chosen in a symmetric manner to simplify the detailed balance condition. The gaussian parameter for generating each of these moves is selected to maintain acceptance ratios between 0.2 and 0.6. We bias our simulations between $Q_4 = 0$ and $Q_4 = 1$ with windows at intervals of 0.025. Finally, simulations are run for 5×10^5 MC steps, with structure convergence existing after approximately 1×10^5 steps but sampling of our Q_4 distributions after 2×10^5 steps.

3 Results

Before performing umbrella sampling, we must determine the effectiveness of the reaction coordinate Q_4 at being able to bias simulations into different structures. Figure 1 shows a range of

structures generated with the added harmonic bias potential at different biasing points. There is a clear distinction in the possible structures that can be realized by biasing along this structure, and so it was selected for use in our umbrella sampling scheme. Other order parameters were investigated, including both higher order Q terms and the number of bonded neighbors, however these failed at being able to effectively generate the different structures of interest. This can best be understood by considering the case of the vesicle, where core particles sit in a very different structure than shell particles. This requires the reaction coordinate selected to be robust to this dichotomy, otherwise by biasing simulations this complex structure may never be realized. For this example however, Q_4 as we've defined it yields a roughly equivalent value between the exterior and interior particles, thus allowing for biased simulations to drive vesicle formation.

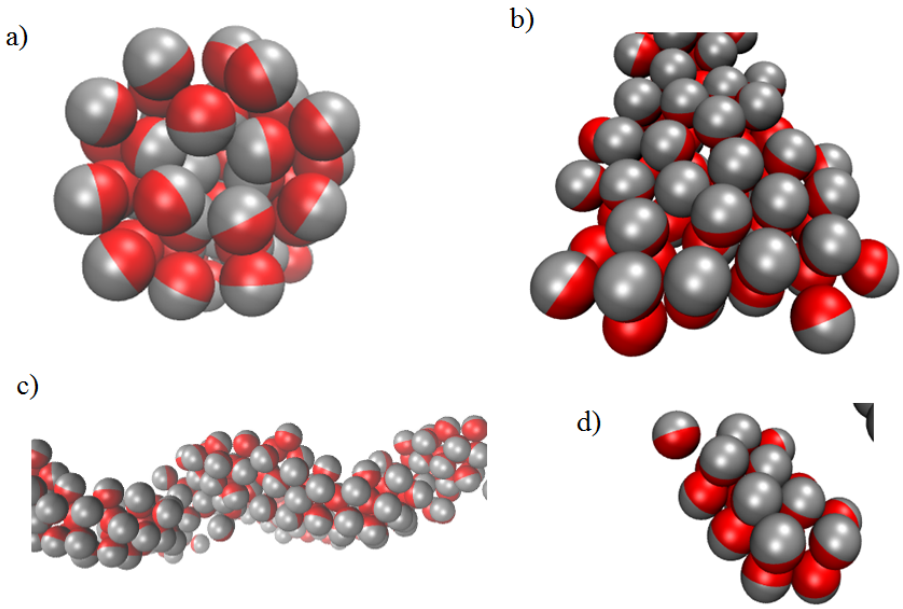

Figure 1: Visualizations for a) cross-section of vesicle, b) planar sheet, c) tube, and d) micelle structures determined from biasing simulations at $Q_4 = 0.3$,0.6,0.75, and 0.9 respectively.

We perform our umbrella sampling over the range $Q_4 \in [0, 1]$, sampling in intervals of 0.025. Our reconstruction is then performed over this same range using the WHAM algorithm. This process is performed for a sequence of different effective temperatures and densities in the gas phase, where the vesicle formation process is of interest. In order to understand the free energy landscape for these varying parameters, it is important to understand the breakdown of structures generated from biasing at different Q_4 values.

In order to determine the ranges relating our reaction coordinate to aggregate structure, we use a technique to compare clusters as developed in [7]. For this, we select several versions of each structure between vesicles, sheets, tubes, and micelles, and decompose these structures into the underlying adjacency graphs that encapsulate the particle bonds in the cluster. We then run a large number of simulations of varying Q_4 values with a large spring constant in the harmonic potential to effectively keep the simulation trajectories close to the bias parameter. From each of these simulations, we take the final system state after reaching equilibrium and decompose the snapshots into their adjacency graphs. We compare these graphs using the IsoRank algorithm [8] to our archetypal structures. IsoRank is a graph matching algorithm which defines a permutation h

that transforms one graph into another in an attempt to minimize the distance between two graphs G_1 and G_2, measured as:

$$dist(G_1, G_2) = ||G_1 - hG_2h^T||_F^2 \tag{14}$$

Where $||.||_F$ is the Frobenius matrix norm. We characterize each biased simulation by the smallest distance to one of our archetypal structures, and we develop approximate ranges for each of these structures across the range of Q_4 from zero to one. This is not an exact process, as sometimes simulations will not map exactly between the bias point and the expected structure, and because of this the relative ranges we have developed can only be considered approximate. The hardest region to classify would be the variation between sheet and tube structures, as much of the range corresponding to sheets can equally spawn tube structures.

From an extensive look at different generated structures from biased simulations, the following four regions have been roughly discerned. For $Q_4 < 0.45$, we see the formation of primarily vesicle type structures; for $0.45 < Q_4 < 0.8$, we see either sheet or tube structures, with tube structures generally existing on the higher end of this region; for $0.8 < Q_4 < 0.95$, we see micelle formations and finally for $Q_4 > 0.95$, we see free particles. Knowing these regimes, we can better understand the free energy landscapes in terms of the approximate structures at each point.

We first look to investigate the effect of temperature on the free energy landscape. Figure 2 shows the free energy plotted as a function of Q_4 at constant density. In this system, we see that in the high temperature regime, corresponding to low values of β, that there is a significant barrier to micelle formation, as particles look to remain in the dilute gas. This barrier is on the order of $2\epsilon - 4\epsilon$ depending on temperature. Once micelles have formed, there is a thermodynamic driving force for either disassembly back into the gas phase or for the generation of more complex aggregate structures. The equilibrium state varies additionally with temperature, where at low β the free particle is on the order of ϵ lower in energy than the aggregate phase, while at high β, the aggregate phase is roughly $5\epsilon - 8\epsilon$ lower in energy than micelles and free particles.

Further, we see a broadening and smearing of the free energy landscape as the temperature increases. For low temperatures, we see a double well phenomenon where micelles should form into two stable phases, either the sheet structure or the vesicle structure. The configuration of bilayer sheets is slightly more stable at these elevated temperatures, however as the temperature decreases, the barrier between sheet and vesicle structures is reduced and vesicle structures become more energetically favorable. Further, as tube structures tend to exist near a region of $Q_4 \approx 0.75 - 0.8$, we see there is a direct energetic driving force for the aggregation of micelles into tubes, and the rearrangement of tubes into vesicles.

Next, we look at the effect of varying system density on the assembly behavior of these Janus particles. Figure 3 shows the free energy landscape in our Q_4 coordinate for a constant temperature system with varying densities all residing in the gas phase. We see that for increases in density, we do not see a drastic shift in the assembly behavior though there are general trends worth noting. First, the barrier for micelle formation is reduced at higher densities, as would be expected due to the increased probability of particle collisions. For all of these investigated systems, it is clear that there is a driving force for the formation of large complex aggregate structures over free particles in solution. Finally, the energy barrier between sheet like structures and vesicles is reduced at low density, as would be expected as the spanning sheet structure should be more difficult to form as the simulation box expands.

One concern with this data is the predicted lower energy state for the bilayer sheet structure. At the investigated density of $\rho\sigma^3 = 0.05$, the sheet structure creates a spanning network across the simulation box, thus increasing the number of bonds in the system by creating a self-interaction. This effectively "infinite" structure should be non-physical in the gas phase, as the relative diluteness

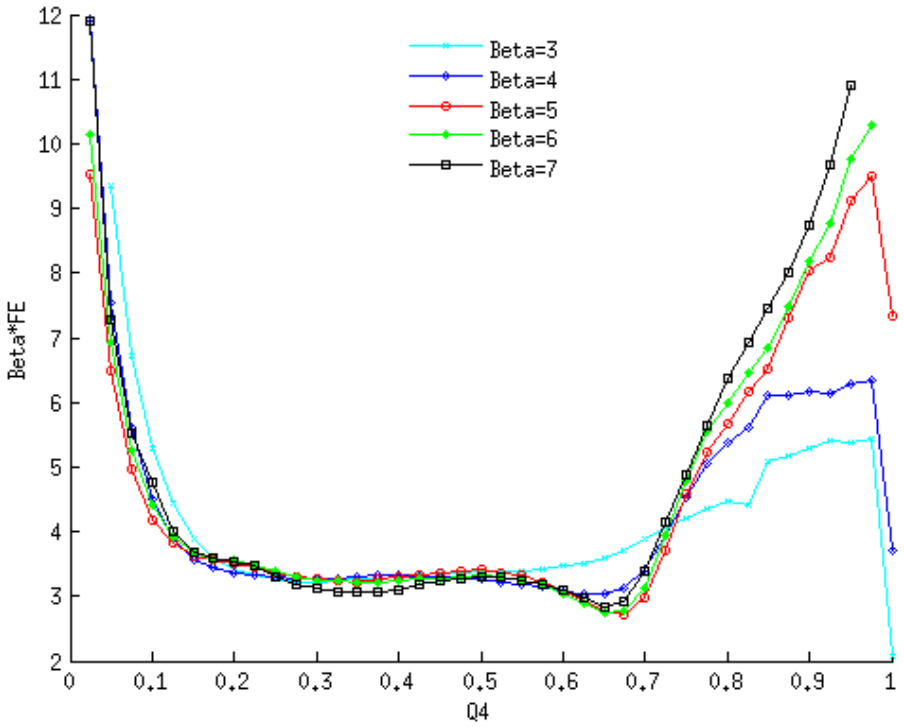

Figure 2: Plot of the free energy as a function of Q_4 for different values of β at a constant density of$\rho\sigma^3 = 0.05$.

of the system is well below the site-percolation density for this planar lattice projected in three dimensions. Further, the low density would starve such an excessively large aggregate from forming due to the low probability of collisions between free particles and the large spanning network. For the purposes of this work, however, we are able to recreate the expected phenomena from [1], where particles in solution have a barrier to micelle formation, upon which these micelles are thermodynamically driven to coalesce and form vesicle structures.

4 Conclusion

We have shown that we can effectively model the free energy landscape for Janus particle self-asembly in the gaseous phase using umbrella sampling and the WHAM algorithm. We see that at high temperatures, there is an activation barrier that must be crossed for particles in the gas to come together and form micelles, after which there is a thermodynamic driving force for vesicle formation. We can effectively reduce this initial barrier by increasing the particle density in our self-assembly system, thus allowing for a higher propensity for vesicle formation. We have found a means to characterize the relative strength of these vesicles as compared to free particles in the gas, thus allowing for possible design of disassembly triggers for a wealth of applications including targeted drug delivery.

Future work in this area would include the use of Grand canonical or Gibbs canonical type moves that would allow for particle addition and deletion or volume moves that could more easily bring the simulations to equilibrium with respect to the reaction coordinate. Additionally, the use of a cluster-order parameter as used by [3] instead of a bond-order parameter would allow for easier

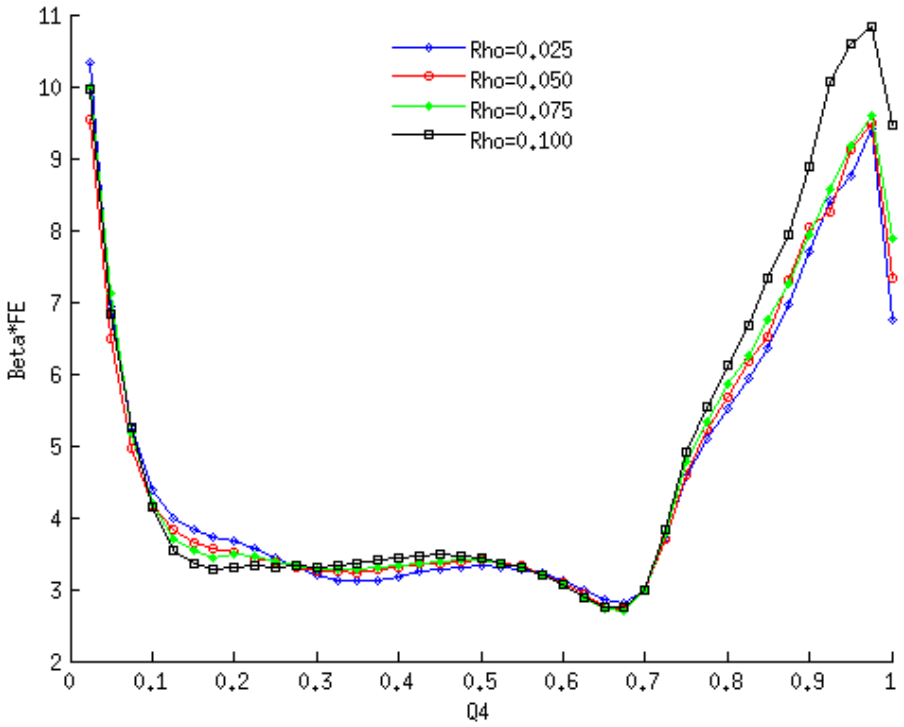

Figure 3: Plot of the free energy as a function of Q_4 for different values of $\rho\sigma^3$ at a constant $\beta = 5$.

derivation of the relative structure along our order parameter as well as more reliable formation of structures from our biasing simulations. Finally, to simplify and speed up our calculations, the use of the generalized geometric cluster algorithm [9] will allow us to nucleate clusters in a fewer number of MC steps, as well as allow for easier cluster reformation.

References

[1] Sciortino, F. et al., Phys. Chem. Chem. Phys., 12 (2010) 11869-11877.
[2] Roux, B., Comp. Phys. Comm., 91 (1995) 275-282.
[3] ten Wolde, P. R. et al., J. Chem. Phys., 104 (1996) 9932-9947.
[4] Fillion, L. et al., J. Chem. Phys., 133 (2010) 244115-244130.
[5] Steinhardt, P. J. et al., Phys. Rev. B, 28 (1983) 784.
[6] Kästner, J., WIREs Comput. Mol. Sci. 1 (2011) 932–942.
[7] Long, A. W. and Ferguson, A. L., In preparation.
[8] Singh, R. et al., Proc. Natl. Acad. Sci. USA, 105 (2008) 12763-12768.
[9] Luijten, E., Comp. in Sci. Eng., 8 (2006) 20-29.